

Anomalies in the Solubility of Alkanes in Near-Critical Water

Clare McCabe,^{*,†} Amparo Galindo,[‡] and Peter T. Cummings^{§,⊥}

Department of Chemical Engineering, Colorado School of Mines, Golden, Colorado 80401; Department of Chemical Engineering and Chemical Technology, Imperial College London, South Kensington Campus, London SW7 2AZ, UK; Department of Chemical Engineering, Vanderbilt University, Nashville, Tennessee, 37235; and Chemical Sciences Division, Oak Ridge National Laboratory, Oak Ridge, Tennessee, 37831

Received: May 6, 2003; In Final Form: August 26, 2003

Recent theoretical and simulation studies suggest an unexpected shift in the solubility of *n*-alkanes in near-critical water, which would indicate that longer *n*-alkane molecules are more soluble than shorter ones. This trend is contrary to what one finds at ambient conditions, where longer alkanes generally have a lower aqueous solubility. The latter is usually interpreted as a consequence of the greater hydrophobicity of longer chains. There is also evidence that the reversal in the solubility close to the critical region may disappear at temperatures well above the critical point. We investigate these phenomena using a simplified version of the statistical associating fluid theory (SAFT) in which molecules are modeled as associating chains of hard-sphere segments with van der Waals mean-field dispersion interactions. Within the SAFT approach it is possible to take into account explicitly the extensive hydrogen bonding present in water and in aqueous solutions as well as the chainlike nature of the *n*-alkane molecules. Both of these features cause anisotropies in the molecular interactions and are responsible for the large nonideality of these systems. The SAFT-HS calculations are compared with available molecular dynamics simulations in an effort to further explore and understand this unexpected behavior. While the SAFT and simulation results agree concerning the reversal and rereversal seen in the Gibbs free energy of solvation (and equivalently the Henry's law constant), the SAFT results suggest that this is not related to changes in alkane solubility, since according to the SAFT calculations the alkanes and water are miscible at the temperature and pressure at which reversal and rereversal of the Gibbs free energy take place.

Introduction

The solubility of organic molecules in aqueous solution is of interest in chemical, biological, and environmental systems. Traditionally, in the petrochemical industry, in the design and operation of plant equipment, the solubility of hydrocarbons in water at each step in the process is needed to trace the phase distribution of the organic species through the entire operation. Aqueous solutions at supercritical conditions have also attracted considerable attention in recent years due to the potential use of supercritical water as a solvent and reaction medium (particularly for supercritical water oxidation of hazardous organic waste^{1,2}). Furthermore, after the discovery of thermophilic organisms in deep-sea hydrothermal vents and geothermal hot springs, new theories suggesting that life may have originated in deep sea vents have been postulated,^{3–7} which provide further motivation for understanding the behavior of organic molecules in high-temperature, high-pressure water, particularly the solubility of more complex organic molecules.

Because of the difficulties involved in performing experimental solubility measurements at supercritical water conditions (the critical point of water is located at 647 K and 220 bar), there has been significant effort in developing equations of state (EOSs) for aqueous organic solutions. In particular, a number

of recent works have been concerned with developing equations for infinite dilution partial molar volumes, which are of special interest in environmental and geochemical systems. These approaches take advantage of the fact that the fluctuation solution theory of Kirkwood and Buff^{8,9} provides a direct relationship between the infinite dilution partial molar volumes and the macroscopic thermodynamic properties of the solvent. Unfortunately, these methods are usually limited by knowledge of the standard thermodynamic properties at the conditions of interest (rarely available at high pressure and temperature). Yezdimer et al.¹⁰ have tackled this issue by developing a functional group approach to predict standard properties. Combining the predicted standard properties with the Kirkwood–Buff (KB) fluctuation theory, they obtain an EOS for infinite-dilution aqueous systems (KB-EOS) and predict partial molar volumes, heat capacities, hydration enthalpies, and Gibbs energies at infinite dilution as well as calculate the chemical potentials of a number of acyclic organic solutes at high temperature and pressure. The predicted Gibbs free energies of hydration ΔG^{hyd} for a series of *n*-alkanes from methane to *n*-heptane indicate that ΔG^{hyd} increases as the chain length of the *n*-alkane increases, as could be expected since the ΔG^{hyd} is a measure of how much energy is required to transfer a molecule from the ideal gas standard state to an aqueous solution at the same conditions. However, at temperatures close to the solvent's critical point, ΔG^{hyd} of the longer *n*-alkanes is found to be lower than that of the shorter *n*-alkanes. This unexpected result would suggest that close to the critical point of water longer *n*-alkane

[†] Colorado School of Mines.

[‡] Imperial College London.

[§] Vanderbilt University.

[⊥] Oak Ridge National Laboratory.

* Corresponding author. E-mail: cmccabe@mines.edu.

molecules are more soluble than shorter ones. They also note a maximum in ΔG^{hyd} as a function of temperature in all water + *n*-alkane systems, which would indicate a minimum in the solubility of *n*-alkanes in water at lower temperatures; computer simulations and previous experimental work confirm the existence of these maxima (see ref 11 and references therein). Although characteristic of aqueous solutions, it is important to recognize that most solvent–solute pairs exhibit such a maximum at least at ambient pressure.^{12,13} As we will see later, it is not always the case that this maximum is directly relevant to the mutual solubility of two components in phase equilibrium. A corollary of this is that relative magnitudes of ΔG^{solv} may not be relevant to relative solubility.

Although more computationally demanding than equation-of-state calculations, molecular simulation is becoming increasingly viable as a route to phase equilibria. Economou and co-workers^{11,14,15} carried out Monte Carlo simulations using the Widom test particle insertion method to obtain Henry's law constants, $K_{H,i}$, and performed Gibbs ensemble Monte Carlo (GEMC) simulations to calculate the high-pressure phase equilibria in methane + water, ethane + water, *n*-butane + water, and *n*-hexane + water mixtures and compared the results with experimental data and with EOS calculations. In the simulations they use an extended simplified point-charge model for water (SPC/E) and a modified version of this potential (MSPC/E) which is specifically reparametrized using properties of water at high temperature. The united atom representation of Smit et al.¹⁶ was used to model the alkane molecules. They consider a wide range of temperature conditions, from 300 to 570 K for methane and ethane in water and from 300 to 460 K in the case of butane and hexane, at pressures close to the corresponding saturation pressure in each case. The simulations predict a maximum in the Henry's law constant (directly related to the ΔG^{hyd}) for the four systems studied, in agreement with experimental data and with the calculations of Yezdimer et al.;¹⁰ unfortunately, the authors do not comment on the reversal of solubility close to the critical point. The simulated high-pressure phase equilibria of methane and ethane in water¹¹ was compared with experiment and with three EOS models (the Soave–Redlich–Kwong, SRK;¹⁷ the associated perturbed anisotropic chain theory, APACT;¹⁸ and the statistical associating fluid theory of Huang and Radosz, SAFT¹⁹). To evaluate the predictive power of the EOS methods, no adjustable binary intermolecular parameters were used. They observe reasonable agreement between the EOS predictions and experimental data at temperatures far below the critical point of water, but not in the high-temperature region. Water + alkane systems are highly nonideal, and as expected, it is necessary to incorporate adjustable intermolecular binary parameters in order to obtain accurate descriptions of their phase behavior using EOS models.^{14,20–23} In later work,¹⁴ a detailed analysis of the Henry's law constant, and its contributions, was carried out comparing a methane + water mixture and a methane + hexadecane mixture. In both systems a maximum in the Henry's law constant $K_{H,i}$ is observed, which is driven by the nonideal contribution of mixing solute and solvent. The EOS models used in ref 14 incorporate an adjusted intermolecular binary parameter for the methane + water mixture, but the authors note that none of the models considered is able to reproduce the maximum in $K_{H,i}$ as a function of temperature. They conclude that EOS models are not able to correlate experimental data for light hydrocarbons in water for the entire temperature range. As we will see later in our work, however, a simplified version of the SAFT approach turns out to be a useful tool, not only to predict

the phase behavior of water + *n*-alkane systems²⁰ but also to examine the infinite dilution properties of these systems.

As mentioned earlier, using the KB-EOS, Yezdimer et al.¹⁰ identified a crossover in solubility as a function of chain length in *n*-alkane + water systems at temperatures around 640 K; this was indicated by a reversal in the relative values of the ΔG^{hyd} (or, equivalently, in the values of $K_{H,i}$). Motivated by this prediction and mindful of the lack of experimental measurements under these difficult conditions, Yezdimer et al.^{24,25} performed molecular dynamics simulations of infinitely dilute solutions of butane and octane in high-pressure, high-temperature water. In these simulations they use the TIP4P-FQ fluctuating point-charge model of Rick et al.²⁶ for the water molecules and the united atom model of Martin and Siepmann²⁷ for the alkane molecules, together with the usual Lorentz–Berthelot combining rules to determine the unlike intermolecular parameters. They calculate ΔG^{hyd} for each of the water + *n*-alkane systems at different temperatures (including the supercritical region) at a fixed pressure of 28 MPa and carry out a comparison with their EOS. The simulation results confirm the predictions of the KB-EOS, indicating that at near-critical conditions the trends in the free energy of hydration, and hence in Henry's law constant, of *n*-alkanes in water reverse, and lower values of ΔG^{hyd} are observed for larger molecules. This would imply that at high temperatures, close to the critical point of water, longer alkanes are more soluble than shorter ones, which is opposite to what is seen at ambient conditions. Using a virial expansion of the free energy of hydration, Yezdimer et al. suggested that the free energies of solvation as a function of chain length would recross at temperatures above the critical temperature. The simulation results agree with this suggestion but have too much statistical noise to unequivocally confirm this prediction.

In this work, we make use of a simplified version of the SAFT approach to study the infinite dilution solubility of butane and octane in water as a function of temperature. This approach was used previously²⁰ to investigate the phase behavior of water + *n*-alkane solutions, but the infinite dilution properties of the systems were not considered. The approach was shown to be useful in a truly predictive sense, in terms of the phase behavior of the mixtures. Our interest now is to see whether this EOS model will also predict the anomalies suggested for these aqueous systems. In addition to this, the molecular basis of the approach allows a systematic investigation of related model systems, which will help in understanding the unusual phenomena.

Theory and Potential Models

The SAFT equation of state stems from the thermodynamic perturbation theory of Wertheim for associating fluids.^{28–31} It was developed in the late 1980s by Chapman and co-workers^{32,33} and has become one of the most widely used and versatile equations of state for the study of fluid phase equilibria.^{34,35} In the SAFT framework molecules are modeled as chains of tangentially bonded spherical segments, which can interact through dispersion and association interactions. The Helmholtz free energy A of a mixture can be written as the sum of various contributions as

$$\frac{A}{NkT} = \frac{A^{\text{ideal}}}{NkT} + \frac{A^{\text{mono}}}{NkT} + \frac{A^{\text{chain}}}{NkT} + \frac{A^{\text{assoc}}}{NkT} \quad (1)$$

where N is the number of molecules, k the Boltzmann constant, and T the temperature and where the superscripts ideal, mono,

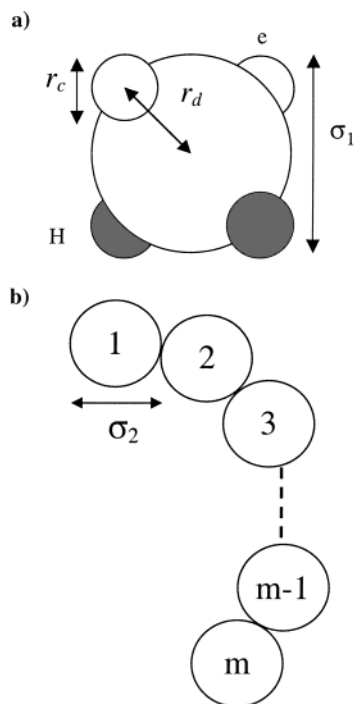


Figure 1. SAFT-HS model for (a) water and (b) *n*-alkanes.

chain, and assoc refer to the ideal, monomer, chain, and association free energy contributions, respectively. The approach is ideally suited to model chain molecules, such as hydrocarbons, as well as hydrogen-bonding fluids, such as water. Many modifications and variations on the original expressions have been proposed and have recently been reviewed in two excellent journal articles.^{34,35} In this work we use the simplified SAFT hard-sphere (SAFT-HS) approach, in which the molecules are modeled as chains of tangent hard-sphere segments with van der Waals mean-field dispersion interactions.

We have chosen to study the infinite dilution behavior of water + butane and water + octane binary mixtures using the simplified SAFT-HS approach, rather than a more sophisticated version of the theory for two reasons: First, in the SAFT-HS approach it is possible to model the phase behavior of different *n*-alkane molecules by taking into account only the difference in molecular chain length. While a parameter *m* takes into account the number of spherical segments in the model corresponding to each *n*-alkane molecule, all other parameters (the size of the spherical segments and the segment–segment mean-field energies) remain fixed. Such a transferable approach is useful in studying the effect of the molecular interactions on the phase behavior without the conflicting influence of the potential model parameters. Second, the SAFT-HS approach is particularly suited to the study of strongly associating fluids, like water, as the hydrogen-bonding interactions mask the simplified description of the weaker dispersion forces.³⁶ For example, the high-pressure behaviors of aqueous mixtures of *n*-alkanes²⁰ and nonionic surfactants,^{37,38} and of hydrogen fluoride mixtures,³⁹ have been successfully modeled using this equation.

In the SAFT-HS approach the water molecules are modeled with a hard spherical repulsive core of diameter σ_1 , with four embedded off-center square well bonding sites (see Figure 1a). Two of the bonding sites account for the electron lone pairs (e) and two for the hydrogen atoms (H) of the water molecule; only e–H bonding is allowed. The sites are placed a distance r_d from the center of the hard core and have a cutoff range r_c ; when the distance between e and H sites is less than r_c , a site–site

attractive interaction energy $\epsilon_{11}^{\text{HB}}$ occurs. This is intended to mimic the short-range directional hydrogen-bonding interactions that dominate the physical properties of aqueous systems. In the case of the *n*-alkane molecules (Figure 1b), a simple united-atom chain model is used in which *m* hard spherical segments of equal diameter σ_2 are tangentially bonded to form a fully flexible chain. A simple empirical relationship between the number of carbon atoms *C* in the alkyl chain and the number of spherical segments *m* in the model was proposed in earlier work: $m = (C - 1)/3 + 1$.^{40,41} A value of *m* = 2.0 thus corresponds to butane, while *m* = 3.33 for octane in this work. Water–water, alkane–alkane, and alkane–water dispersion interactions are incorporated at the mean-field level of van der Waals using parameters ϵ_{11} , ϵ_{22} , and ϵ_{12} , respectively.

The pure-component parameters for water used here were obtained in earlier work by fitting to experimental vapor-pressure and saturated liquid density data from the triple to the critical point.²⁰ The size and mean-field energy parameters have been rescaled using the experimental critical temperature and pressure of water (647 K and 220 bar) since the near-critical region is of special interest here. The final intermolecular parameters used are (see Galindo et al.²⁰ for more details): $\sigma_1 = 3.589 \text{ \AA}$, $\epsilon_{11}/k = 4384 \text{ K}$, $\epsilon_{11}^{\text{HB}}/k = 1534 \text{ K}$, and $r_c/\sigma_1 = 0.679$ (the corresponding bonding volume K/σ_1^3 for this cutoff range is 0.0292). The parameters for the *n*-alkanes are obtained by fitting the calculated critical point of a model molecule with *m* = 2 to the experimental critical temperature and pressure of *n*-butane (425 K and 37.97 bar), resulting in segment parameters $\sigma_2 = 3.802 \text{ \AA}$ and $\epsilon_{22}/k = 2954 \text{ K}$. In the SAFT-HS approach these segment parameters are then used in a transferable way to study other members of the *n*-alkane homologous series; i.e., to obtain the thermodynamic properties of other *n*-alkanes, only the length of the hydrocarbon chain changes through the parameter *m*, with all other parameters unchanged.

In the study of mixture phase behavior the Lorentz–Berthelot combining rule is typically used to determine unlike or cross interaction parameters from pure component parameters. In the case of water + *n*-alkane systems in the SAFT-HS approach, the unlike size σ_{12} and dispersion energy ϵ_{12} parameters need to be specified. The Lorentz or arithmetic mean used to determine σ_{12} is exact in the case of hard-sphere models; however, the Berthelot or geometric mean used to determine ϵ_{12} is not adequate for highly nonideal mixtures. A binary interaction parameter k_{ij} must be introduced which modifies the dispersion interaction so that $\epsilon_{12} = (1 - k_{ij})(\epsilon_{11}\epsilon_{22})^{1/2}$. The value of k_{ij} is determined by comparison with experimental mixture data. In previous work,²⁰ this parameter was optimized in order to provide an accurate representation of the critical point in a water + *n*-butane mixture at 38 MPa; a value of $k_{ij} = 0.14$ was found. It was shown that SAFT-HS could be used as a predictive approach by transferring this unlike parameter to predict the phase behavior of the mixture in a wide range of temperatures and pressures as well to study the phase behavior of other binary mixtures of the same homologous series. Using this simple approach, very good agreement was obtained between the SAFT-HS predictions and experimental data for the high-pressure critical lines of a series of water + *n*-alkane systems. In this work we adopt the same transferable approach, using the same value of the unlike parameter ($k_{ij} = 0.14$), to investigate the effect of chain length and temperature on the infinite dilution properties of *n*-alkanes in water.

Infinite Dilution Properties

Before presenting our results, it is useful to review briefly some fundamental concepts. The infinite dilution phase behavior

can be studied through the calculation of the Henry's law constant of a solute j in solvent i

$$K_{H,j,i} = \lim_{x_j \rightarrow 0} \left(\frac{f_j}{x_j} \right) \quad (2)$$

where f_j is the fugacity of the solute and x_j its mole fraction. Note that this definition suggests that larger values of $K_{H,j,i}$ correspond to lower solubility of solute j in solvent i , and vice versa.¹³ This is also reflected in the relation between the Henry's law constant and the excess Gibbs free energy of hydration $\Delta G^{\text{hyd}}(T,P)$ in the form introduced by Ben-Naim⁴²

$$\ln \left(\frac{K_{H,j,i}}{\rho_i N k T} \right) = \frac{\Delta G^{\text{hyd}}(T,P)}{N k T} \quad (3)$$

where ρ_i is the number density of the solvent and ΔG^{hyd} is the change in free energy when a solute is inserted at infinite dilution in a fixed position in the pure solvent (at constant pressure) at temperature T and pressure P . This relation can also be written in terms of the Ostwald solubility coefficient γ ¹³ by

$$\Delta G^{\text{hyd}} = -N k T \ln \gamma \quad (4)$$

since $\gamma = \rho_i N k T / K_{H,j,i}$. As defined, ΔG^{hyd} is equal to the residual chemical potential of the solute at infinite dilution

$$\Delta G^{\text{hyd}}(T,P) = \mu_j^{\text{res},\infty}(T,P) \quad (5)$$

and accounts directly for the interactions between the solute and the solvent. Thus, it can be obtained in computer simulation calculations using the Widom test particle insertion method,⁴³ or from the Helmholtz free energy through the standard thermodynamic relation

$$\mu_j = \left. \frac{\partial A}{\partial N_j} \right|_{T,V,N_i \neq j} \quad (6)$$

We use the SAFT-HS approach²⁰ together with the relations in this section to study the infinite dilution phase behavior of two water + n -alkane binary mixtures.

Results

We consider two binary mixtures: water (1) + n -butane (2) and water (1) + n -octane (2), and calculate the phase behavior and infinite dilution properties at a constant pressure of 28 MPa; the choice of pressure follows from the work of Yezdimer et al.¹⁰ A detailed analysis of the phase behavior of water + n -alkane systems using the SAFT-HS approach can be found in ref 20, while comparisons of different association equation-of-state models have been presented by a number of authors.^{22,23} The phase behavior of water + n -alkane binary mixtures is characterized by the large degree of liquid–liquid phase separation, which, at high pressure, persists up to temperatures close to the critical temperature of water. Two Tx slices of the water (1) + n -butane (2) and water (1) + n -octane (2) phase diagrams at a constant pressure of 28 MPa as calculated with the SAFT-HS approach are shown in Figure 2. The extreme immiscibility between the two components is evident from the figure, where a large region of liquid–liquid separation is observed. (The compositions of the water-rich phases for varying temperatures are better seen in Figure 2b.) The immiscibility increases at lower temperatures and decreases at higher temperatures, disappearing at a liquid–liquid critical point close to the critical temperature of water. At 28 MPa the water +

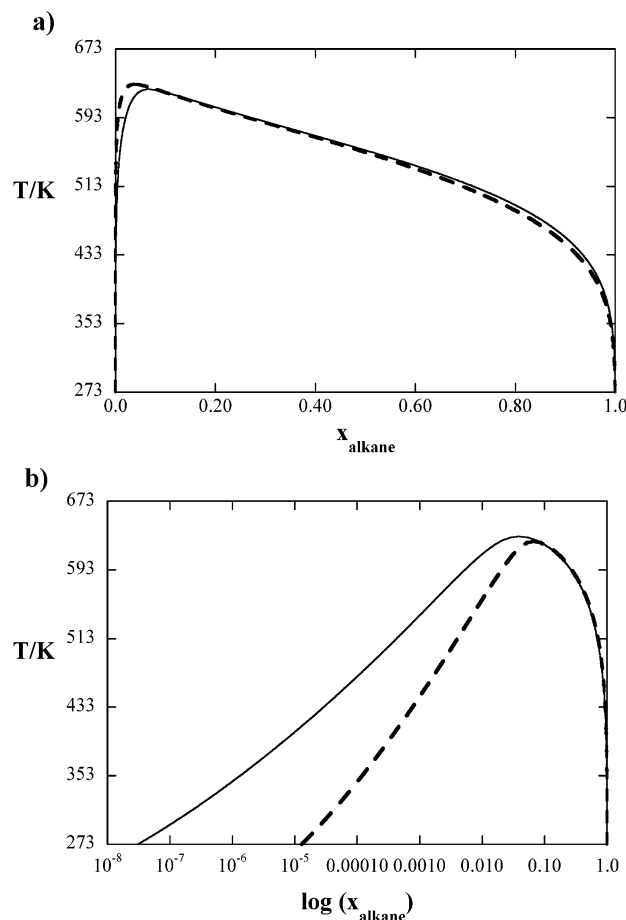


Figure 2. SAFT-HS predictions of the water (1) + butane (2) (solid line) and water (1) + octane (2) (dashed line) phase behavior at a constant pressure of 28 MPa.

n -butane binary mixture first becomes miscible at 626 K, while in the water + n -octane mixture the critical temperature is 632 K. The water-rich phase contains fewer octane molecules than butane molecules, as could be expected given the larger size of octane. At the lowest temperatures, the difference in n -alkane concentration is significant: the mole fraction of butane in water is 2 orders of magnitude larger than that of octane. Examining the oil-rich phases, it can be seen that the butane-rich phase contains slightly less water than the octane-rich phase for a fixed temperature. This is in agreement with experimental data⁴⁴ and suggests that the phase behavior is being dominated by the mean-field attractive terms. In our model the unlike attractive interactions are modeled per segment, so that the overall attractive interaction is greater between water and octane than between water and butane. In the water-rich phase at low and intermediate temperatures the phase behavior is dominated by the water–water hydrogen bond interactions. It is also noticeable that the solubility of water in the n -alkane phase is orders of magnitude larger than the solubility of the n -alkane in the water-rich phase and that the theoretical approach predicts a continuous decrease in solubility for decreasing temperature in both phases. It has long been known that the composition of n -alkane in the water-rich phase increases at low temperatures;⁴⁴ the SAFT-HS approach does not predict this unusual behavior. The reason behind the increase in the equilibrium mole fraction of n -alkane at low temperatures is not yet fully understood; more sophisticated versions of the SAFT approach can be used which are able to reproduce a minimum in the n -alkane mole fraction in the water-rich phase,^{45,46} but they cannot provide a satisfactory

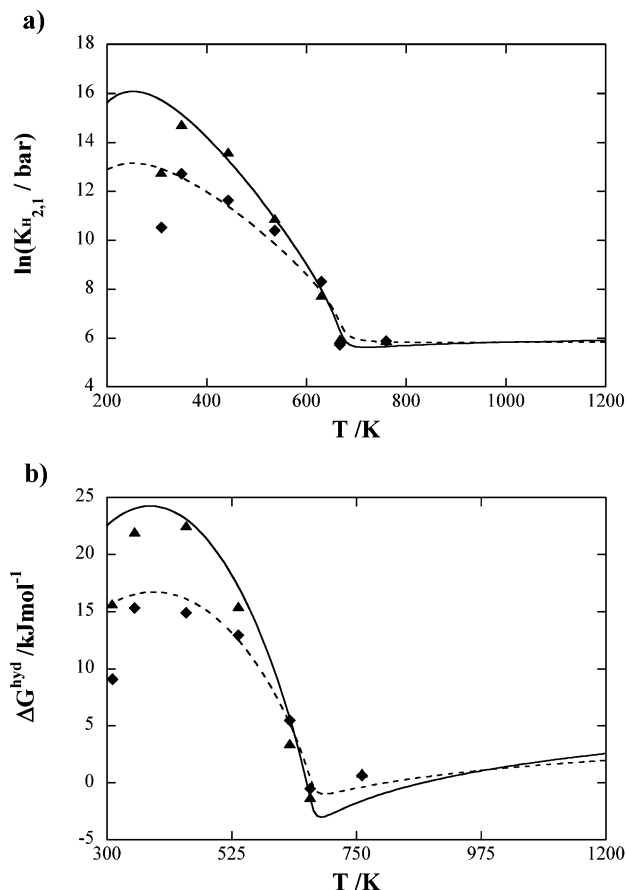


Figure 3. Prediction of Henry's law constant and Gibbs free energy of hydration for butane (solid line) and octane (dashed line) infinitely dilute in aqueous solution at 28 MPa compared to simulation data of Yezdimer et al.⁴⁹

explanation for this behavior. At first one is tempted to relate the minimum in *n*-alkane concentration with the maximum observed in the ΔG^{hyd} , or in $K_{H,2,1}$, which corresponds to a minimum in the Ostwald solubility coefficient γ . However, while the SAFT-HS approach cannot describe the low-temperature concentration minima, it does predict a maximum in ΔG^{hyd} (or a minimum in γ) in good agreement with simulation data (see Figure 3). This seems to indicate that care needs to be taken in establishing a direct relationship between infinite dilution properties and phase coexistence.

In Figure 3 we present a comparison of the Henry's law constant in the water-rich phase, $K_{H,2,1}$, and the excess free energies of hydration ΔG^{hyd} (see eq 3) calculated by Yezdimer et al.^{24,25} using computer simulations with those obtained with the SAFT-HS approach. It is clear from the figures that the SAFT-HS predictions are in excellent agreement with the simulation data. It is useful to recall at this point that the intermolecular parameters used in this work were determined in previous work,²⁰ meaning that no adjustment of the unlike parameter has been carried out in order to reproduce the computer simulation data here; the calculations correspond to a true prediction of the infinite dilution properties of these aqueous mixtures. Both $K_{H,2,1}$ and ΔG^{hyd} are seen to increase with temperature, go through a maximum, and later decrease at the higher temperatures. At temperatures above the critical point of water, a small increase is again seen (see Figure 3b). Errington et al.¹¹ have suggested that these maxima could not be obtained using equation-of-state models, but as shown here, and as obtained with the KB-EOS model of Yezdimer et al.,¹⁰ this is not the case. The maxima in $K_{H,2,1}$ and ΔG^{hyd} correspond

to minima of the Ostwald solubility parameter γ (see eq 4), but we find that this does not correspond to a minimum of the *n*-alkane concentration in the water-rich phase in equilibrium with an *n*-alkane-rich phase. As mentioned, while our SAFT-HS calculations are in good agreement with the simulation data in terms of the low-temperature maximum of the Henry's law constant (and ΔG^{hyd}), the calculation of the fluid phase behavior does not reflect the expected increase in solubility at low temperature. The Henry's law constant is commonly used in engineering applications to determine the solubility of sparingly soluble solutes (whether gases or liquid) in liquid solvents.¹³ For example, a quick estimate of solubilities in oil–water systems is usually carried out by relating the composition of the *n*-alkane in the water-rich phase to $K_{H,2,1}$ applying Henry's law constant and assuming the oil-rich phase to be pure alkane, so that from eq 2

$$x_2 \cong P_2^{\text{sat}}(T)/K_{H,2,1} \quad (7)$$

In deriving this equation it has also been assumed that the saturated alkane vapor is ideal, so that this relation is expected to be more accurate at lower pressures. Although the pressure studied here is rather high (28 MPa), we have also performed calculations at low pressures (0.02 MPa) and observe the same findings. As a conclusion, it seems that for these highly nonideal mixtures it is not possible to estimate accurately the equilibrium compositions of the demixed aqueous phase through the Henry's law constant.

The study of solubility parameters and free energies of hydration can also be useful in estimating relative solubilities. From Figure 3 it can be seen that in the low-temperature range, and up to ~ 630 K, both $K_{H,2,1}$ and ΔG^{hyd} suggest that *n*-butane is more soluble than *n*-octane in the water-rich phase. This is corroborated both by experimental data^{47,48} and by phase equilibria calculations. Unexpectedly, at temperatures close to the critical point of water a reversal in the solubility of these molecules in water is seen which suggests that a larger *n*-octane molecule would be more soluble than a smaller *n*-butane one. As mentioned in the Introduction, this was first predicted by Yezdimer et al. with the KB-EOS¹¹ and later confirmed by computer simulation.^{24,25} The SAFT-HS calculations reflect the same behavior. However, on closer inspection of Figures 2 and 3, it becomes clear that the crossover in the Henry's law constant is not associated with an increased solubility in terms of the phase behavior, as both mixtures are fully miscible at the conditions where the crossover is observed. As before, care needs to be taken in relating infinite dilution and coexistence properties. ΔG^{hyd} corresponds to the excess free energy of inserting a molecule of solute in a fixed position in the solvent, while phase separation is determined by the total free energy of the mixture. The lower values of ΔG^{hyd} observed for longer *n*-alkane molecules (*n*-octane here) compared to shorter *n*-alkanes (*n*-butane here) suggest that in a reaction process in aqueous media the formation of larger hydrocarbon molecules would be favored. It is very interesting to note that this would be in support of the theories of the origin of life having originated in deep-sea vents.^{3–7} At temperatures of ~ 1000 K, both the theoretical approach and the computer simulation data predict the solubility to revert to the expected behavior, with the excess free energy of hydration of *n*-butane molecules being lower than that of *n*-octane molecules. Note that at these high temperatures the lower solubility of octane has a different origin to that observed at low temperatures. We come back to discuss this later. In their work, Yezdimer et al.²⁵ noted that the

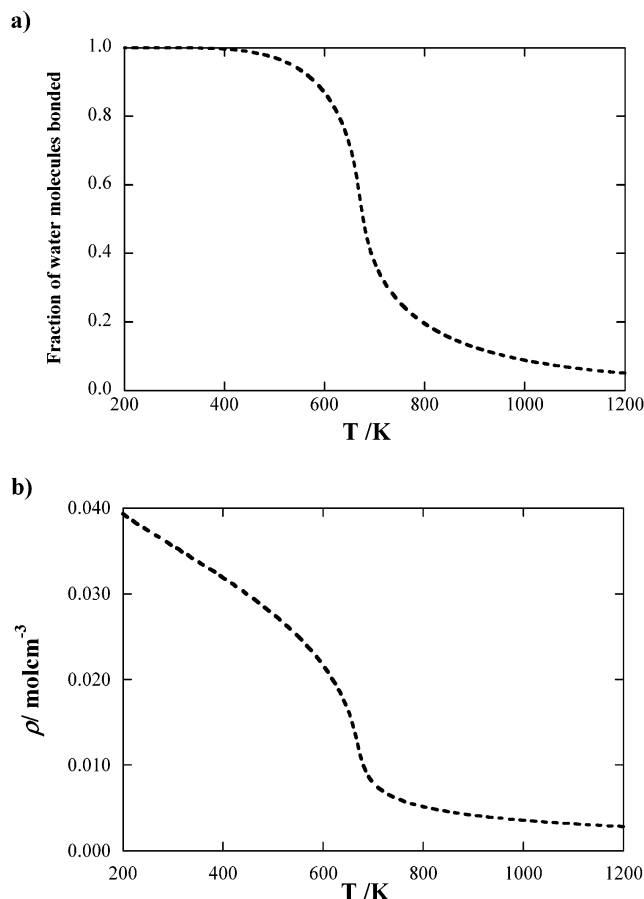


Figure 4. (a) Fraction of water molecules bonded and (b) liquid density as a function of temperature for an infinitely dilute water + alkane binary mixture at 28 MPa.

simulation data suggest that the free energy of hydration is finite and continuous at the critical point; our calculations confirm this. At this point, we can take advantage of the accuracy of the SAFT-HS predictions and of the fact that, as a molecular-based theory, it also provides a useful tool to investigate in detail the molecular origin of the unexpected temperature dependence of the relative solubilities of *n*-alkanes in water.

In the SAFT approach the effect of association interactions, such as hydrogen bonds, on the thermodynamic behavior is explicitly taken into account through short-range attractive interaction sites. In determining the contribution to the free energy due to water–water hydrogen-bond interactions, the fraction of molecules bonded at least one site (see ref 20 for details) can also be obtained. In Figure 4 the fraction of water molecules bonded in the water-rich phase at 28 MPa is presented. It is well-known that hydrogen bonding dominates the phase behavior of aqueous systems at low temperatures, and accordingly, the theoretical calculations indicate that most of the water molecules are bonded. As the temperature increases, the decrease in density (see Figure 4b)) and the increase in thermal energy cause the breakage of the hydrogen bonds. It is noticeable that a rapid change in the number of molecules bonded is observed in the near-critical temperature region, which also corresponds to the temperature region in which the crossover of the alkane solubilities occurs. Following this, in Figure 5 we investigate the effect of changing the strength of the hydrogen bond energy on the Henry's law constant, and the free energy of hydration, for the water + *n*-butane binary mixture. As the strength of the hydrogen bond is reduced, the maxima in $K_{H_{2,1}}$ and ΔG^{hyd} decrease and move toward lower

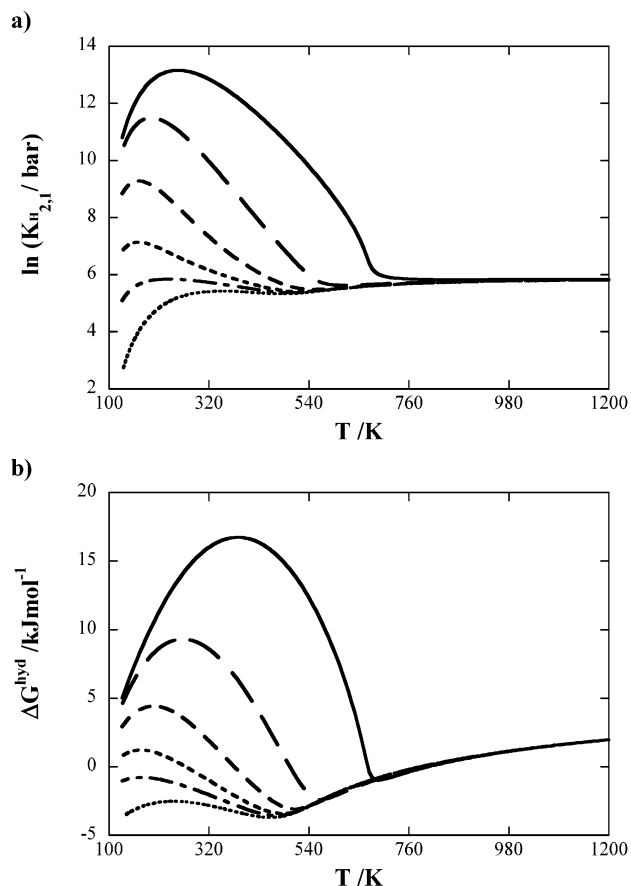


Figure 5. Effect of the diminishing strength ϵ_{HB} of the hydrogen bond on (a) the Henry's law constant and (b) Gibbs free energy of hydration for the infinitely dilute water (1) + butane (2) binary mixture at 28 MPa. From the solid line to the dotted line, $\epsilon_{\text{HB}}/k = 1534$ K (full strength), 767 K (half strength), 383.5 K (quarter), 191.75 K (eighth), 95.875 K (sixteenth), and 0 K.

temperatures (where hydrogenbond interactions are favored). At intermediate temperatures the ΔG^{hyd} is now seen to turn more negative for weaker hydrogen bond interactions, and the process of dissolving a molecule of solute in the solvent becomes favorable. The phase behavior here is dominated by attractive mean-field interactions. At the higher temperatures the curves coincide in a common limit, the hard-sphere limit, where the behavior is driven by the repulsive interactions. As mentioned earlier, *n*-butane is modeled with $m = 2$ tangentially bonded hard-sphere segments with segment–segment dispersion interactions treated at the mean-field level of van der Waals, while *n*-octane molecules are modeled as $m = 3.33$ spherical segments, so that, at the same density and temperature, the water–octane dispersion interaction is larger than the water–butane interaction. In Figure 6 the infinite dilution properties of model *n*-octane and *n*-butane + water systems are compared, and this becomes more evident. When the hydrogen bond interactions dominate (at lower temperatures and large values of $\epsilon_{11}^{\text{HB}}$), more energy is needed to insert an *n*-octane molecule than an *n*-butane one due to the energetic penalty of disrupting the network of water hydrogen bonds. But, for the weakest energies *n*-octane is seen to be more soluble in water than butane for all temperatures below ~ 1000 K due to the larger dispersion interactions of this system. At high enough temperatures the phase behavior is, of course, dominated by the hard-sphere repulsive interactions, and more energy is required to dissolve *n*-octane than *n*-butane.

Before finishing this section, it is useful to add one final comment regarding the *n*-alkane-rich phase and the choice of

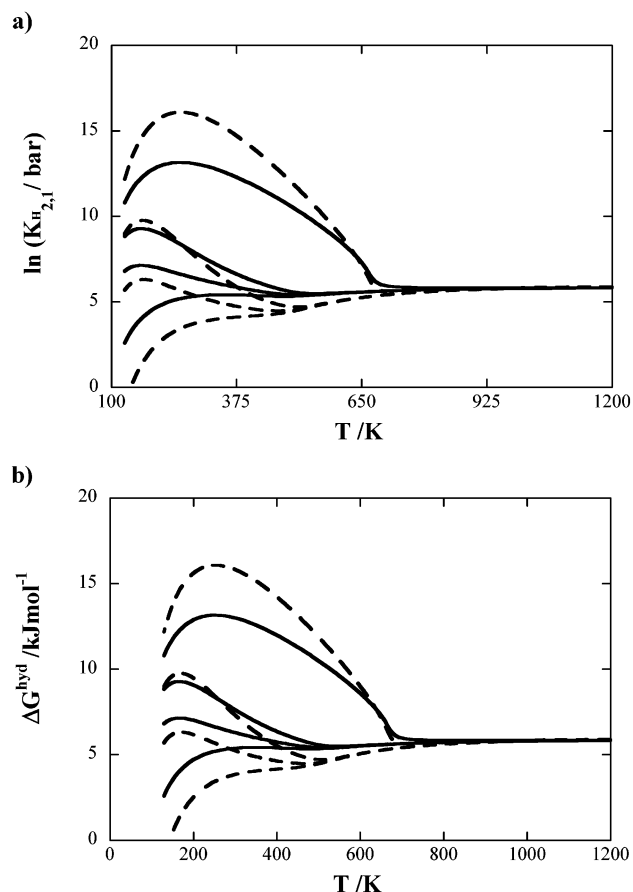


Figure 6. Comparison of the effect of the diminishing strength of the hydrogen bond on (a) the Henry's law constant and (b) Gibbs free energy of hydration for the infinitely dilute water (1) + butane (2) (solid line) and water (1) + octane (2) (dashed line) binary mixtures at 28 MPa. From the highest set of curves to the lowest, $\epsilon_{HB}/k = 1534$ K (full strength), 383.5 K (quarter), 191.75 K (eighth), and 0 K.

reference state in these calculations. We have mentioned that, in terms of the phase behavior, a larger concentration of water is found in the water + *n*-octane system than in the water + *n*-butane system. In Figure 7 the Henry's law constant of water in the oil-rich phase $K_{H2,1}$ and the excess free energy associated with the process of inserting a molecule of water in a fixed position in the *n*-alkane phase ΔG^{hyd} are presented. As can be seen, a comparison of $K_{H2,1}$ for the *n*-butane and *n*-octane mixture would suggest that water is less soluble in *n*-octane, while an examination of ΔG^{hyd} suggests the opposite, in better agreement with the coexistence calculations. In comparing solvents of different density, such as here, it is especially important to bear in mind the reference state as first noted by Ben-Naim.⁴²

Conclusions

We have studied the infinite dilution properties of two water + *n*-alkane mixtures using a simplified SAFT equation of state (SAFT-HS) in which hard-sphere chain molecules with van der Waals dispersion interactions are treated. In previous work,²⁰ the approach was shown to be useful in predicting the critical phase behavior of the homologous series of water + *n*-alkane binary mixtures. In this work, we have used the same intermolecular parameters as in the previous study and find that the infinite dilution properties calculated are in excellent agreement with computer simulation data of the Henry's law constant and free energies of hydration in the water-rich phase. A number of characteristic, as well as unusual, features had been described

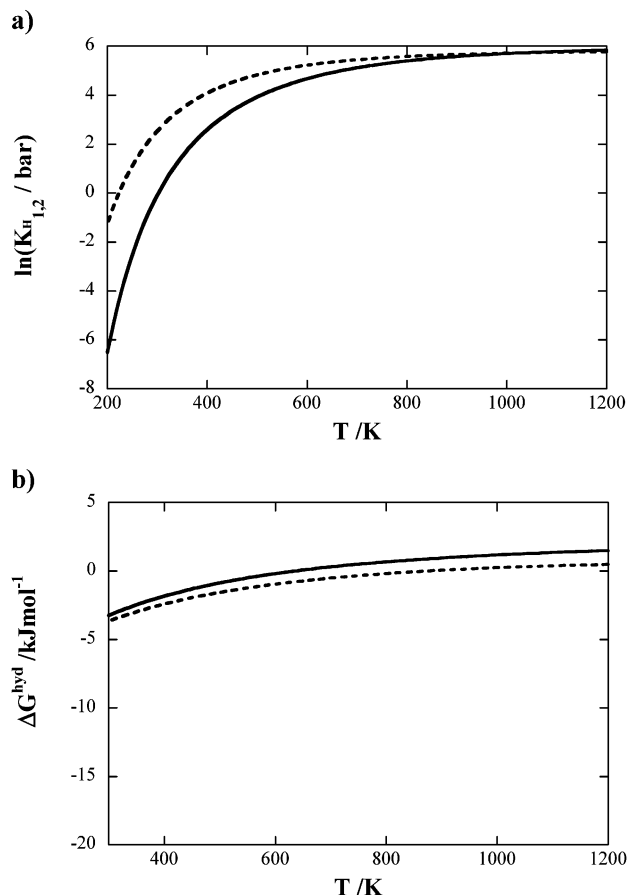


Figure 7. Prediction of the Henry's law constant and the Gibbs free energy of hydration for water infinitely dilute in a hydrocarbon solution at 28 MPa. The solid line corresponds to the water (1) + butane (2) binary mixture and the dashed line to the water (1) + octane (2) binary mixture.

earlier by solution theories of the Kirkwood–Buff formalism¹⁰ and molecular dynamics simulations:^{24,25} a maximum in the Henry's law constant (and in the free energy) present at low temperatures, as in most aqueous solutions, and a crossover in solubility which suggests *n*-octane to be more soluble than *n*-butane are seen at near-critical conditions. The SAFT-HS approach reproduces these trends. One advantage of the approach used here is that it allows also the calculation of the phase behavior of the mixture. We find that it is not always possible to estimate accurately the compositions of the coexisting phases from the Henry's law constants in these nonideal mixtures. In addition, we have investigated the origin of the unusual crossover in solubility and find that it is due to the larger dispersion interactions between water and *n*-octane (as compared to the water–*n*-butane), which dominate in a small temperature region where the temperature is high enough so that little hydrogen bonding takes place, but before the repulsive terms dominate. These findings may be in support of recent theories suggesting the origin of life to have occurred in deep-sea vents as, as shown, larger *n*-alkane molecules are favored over shorter ones in aqueous media. At the highest temperatures, the repulsive contributions dominate, and a rereversal of solubility is observed. The SAFT-HS approach is a simple equation of state; yet, it incorporates the crucial nonideal contributions of these mixtures, such as hydrogen bonding and the chainlike nature of the *n*-alkane molecules. As such, it becomes a very powerful predictive tool for the study of these systems.

Acknowledgment. C.M.C. and P.T.C. were supported by the Division of Chemical Sciences, Geosciences, and Biosciences, Office of Basic Energy Sciences, U.S. Department of Energy, under Grant DE-FG02-03ER15385 to Vanderbilt University. A.G. thanks the EPSRC for the award of an Advanced Research Fellowship. We also thank Eric Yezdimer for numerous discussions and for introducing us to this problem.

References and Notes

- (1) Crain, N.; Shanableh, A.; Gloyna, E. *Water Sci. Technol.* **2000**, 42, 363–368.
- (2) Schmieder, H.; Abeln, J. *Chem. Eng. Technol.* **1999**, 22, 903–908.
- (3) Gottschal, J. C.; Prins, R. A. *Trends Ecol. Evol.* **1991**, 6, 157–162.
- (4) Glasby, G. P. *Episodes* **1998**, 21, 252–256.
- (5) Forterre, P. *Recherche* **1999**, 36–43.
- (6) Di Giulio, M. *Gene* **2000**, 261, 189–195.
- (7) Russell, M. J.; Hall, A. J. In *The Geochemical News*; The Geochemical Society: St. Louis, MO, 2002; Vol. 113.
- (8) O'Connell, J. P. In *NATO Advanced Study Institute on Supercritical Fluids – Fundamentals for Application, July 18–31, 1993, Kemer, Antalya, Turkey*; Levelt Sengers, J. M. H., Ed.; Kluwer: Dordrecht, The Netherlands, 1994.
- (9) Kirkwood, J. G.; Buff, F. P. *J. Chem. Phys.* **1951**, 19, 774–782.
- (10) Yezdimer, E. M.; Sedlbauer, J.; Wood, R. H. *Chem. Geol.* **2000**, 164, 259–280.
- (11) Errington, J. R.; Boulougouris, G. C.; Economou, I. G.; Panagiotopoulos, A. Z.; Theodorou, D. N. *J. Phys. Chem. B* **1998**, 102, 8865–8873.
- (12) Harvey, A. H. *AIChE J.* **1996**, 42, 1491–1494.
- (13) Prausnitz, J. M.; Lichtenthaler, R. N.; Gomes de Azevedo, E. *Molecular Thermodynamics of Fluid-Phase Equilibria*, 2nd ed.; Prentice Hall: Englewood Cliffs, NJ, 1999.
- (14) Boulougouris, G. C.; Voutsas, E. C.; Economou, I. G.; Theodorou, D. N.; Tassios, D. P. *J. Phys. Chem. B* **2001**, 105, 7792–7798.
- (15) Boulougouris, G. C.; Errington, J. R.; Economou, I. G.; Panagiotopoulos, A. Z.; Theodorou, D. N. *J. Phys. Chem. B* **2000**, 104, 4958–4963.
- (16) Smit, B.; Karaborni, S.; Siepmann, J. I. *J. Chem. Phys.* **1995**, 102, 2126–2140.
- (17) Soave, G. *Fluid Phase Equilib.* **1972**, 82, 345.
- (18) Ikonou, G. D.; Donohue, M. D. *AIChE J.* **1986**, 32, 1716–1725.
- (19) Huang, S. H.; Radosz, M. *Ind. Eng. Chem. Res.* **1990**, 29, 2284–2294.
- (20) Galindo, A.; Whitehead, P. J.; Jackson, G.; Burgess, A. N. *J. Phys. Chem.* **1996**, 100, 6781–6792.
- (21) Voutsas, E. C.; Boulougouris, G. C.; Economou, I. G.; Tassios, D. *Ind. Eng. Chem. Res.* **2000**, 39, 797–804.
- (22) Economou, I. G.; Tsonopoulos, C. *Chem. Eng. Sci.* **1997**, 52, 511–525.
- (23) Yakoumis, I. V.; Kontogeorgis, G. M.; Voutsas, E. C.; Hendriks, E. M.; Tassios, D. P. *Ind. Eng. Chem. Res.* **1998**, 37, 4175–4182.
- (24) Yezdimer, E. M.; Chialvo, A. A.; Cummings, P. T. *Fluid Phase Equilib.* **2001**, 183, 289–294.
- (25) Yezdimer, E. M.; Chialvo, A. A.; Cummings, P. T. *J. Phys. Chem. B* **2001**, 105, 841–847.
- (26) Rick, S. W.; Stuart, S. J.; Berne, B. J. *J. Chem. Phys.* **1994**, 101, 6141–6156.
- (27) Martin, M. G.; Siepmann, J. I. *J. Phys. Chem. B* **1998**, 102, 2569–2577.
- (28) Wertheim, M. S. *J. Stat. Phys.* **1984**, 35, 19–34.
- (29) Wertheim, M. S. *J. Stat. Phys.* **1984**, 35, 35–47.
- (30) Wertheim, M. S. *J. Stat. Phys.* **1986**, 42, 459–476.
- (31) Wertheim, M. S. *J. Stat. Phys.* **1986**, 42, 477–492.
- (32) Chapman, W. G.; Gubbins, K. E.; Jackson, G.; Radosz, M. *Fluid Phase Equilib.* **1989**, 52, 31–38.
- (33) Chapman, W. G.; Gubbins, K. E.; Jackson, G.; Radosz, M. *Ind. Eng. Chem. Res.* **1990**, 29, 1709–1721.
- (34) Economou, I. G. *Ind. Eng. Chem. Res.* **2002**, 41, 953–962.
- (35) Muller, E. A.; Gubbins, K. E. *Ind. Eng. Chem. Res.* **2001**, 40, 2193–2211.
- (36) McCabe, C.; Galindo, A.; Gil-Villegas, A.; Jackson, G. *Int. J. Thermophys.* **1998**, 19, 1511–1522.
- (37) Garcia Lisbona, M. N.; Galindo, A.; Jackson, G.; Burgess, A. N. *Mol. Phys.* **1998**, 93, 57–71.
- (38) Garcia Lisbona, M. N.; Galindo, A.; Jackson, G.; Burgess, A. N. *J. Am. Chem. Soc.* **1998**, 120, 4191–4199.
- (39) Galindo, A.; Whitehead, P. J.; Jackson, G.; Burgess, A. N. *J. Phys. Chem. B* **1997**, 101, 2082–2091.
- (40) Jackson, G.; Gubbins, K. E. *Pure Appl. Chem.* **1989**, 61, 1021–1026.
- (41) Archer, A. L.; Amos, M. D.; Jackson, G.; McLure, I. A. *Int. J. Thermophys.* **1996**, 17, 201–211.
- (42) Ben-Naim, A. *Statistical Thermodynamics for Chemists and Biochemists*; Plenum Press: New York, 1992.
- (43) Frenkel, D.; Smit, B. *Understanding Molecular Simulation: From Algorithms to Applications*; Academic Press: San Diego, 1996.
- (44) Tsonopoulos, C. *Fluid Phase Equilib.* **1999**, 156, 21–33.
- (45) Patel, B.; Galindo, A. *Ind. Eng. Chem. Res.*, in press.
- (46) Blas, F. J. PhD Dissertation, Universitat Rovira i Virgili, 2000.
- (47) de Loos, T. W.; Wijten, A. J. M.; Diepen, G. A. M. *J. Chem. Thermodyn.* **1980**, 12, 193–204.
- (48) de Loos, T. W.; Penders, W. G.; Lichtenthaler, R. N. *J. Chem. Thermodyn.* **1982**, 14, 83–91.
- (49) Yezdimer, E. M.; Chialvo, A. A.; Cummings, P. T. *J. Phys. Chem. B* **2000**, 105, 841–847.